Thermographic Investigation of Laser Metal Deposition

Sreekar Karnati*, Todd Sparks*, Frank Liou*
*Department of Mechanical and Aerospace Engineering, Missouri University of Science and Technology, Rolla, MO, 65409

Abstract

Primitive stages of studies on and with additive manufacturing techniques popularly involve thin wall geometry. In the current effort attempts were made to capture various thermal aspects during deposition of a thin wall geometry. The thermo-graphic data was captured using a FLIR A615 infrared camera. Post processing using edge detection algorithms and image processing techniques, the geometric and thermal aspects of meltpool and tail of the meltpool were obtained. The effect of geometry and power on shape of the meltpool and its tail were obtained. The depositions of SS 316 with varying power. These observations were discussed and analyzed in aim to perform planned deposition of functionally gradient materials in future.

Introduction

Laser metal deposition (LMD) is a layer by layer additive manufacturing process where a material is added to the substrate in the form of powder or wire and is cladded onto the substrate using a high power energy source, as the name goes a laser. The layer by layer build schema provides the scope to build complex parts and profiles with intricate details. The rapid heating and cooling aspect of the process ensures good mechanical properties and is instrumental in fabricating otherwise not possible non-equilibrium material properties. In order to do so a high degree of control is required over the process parameters such as power, scan speed, powder flow rate, beam size etc.

In order to gain insight into the happening process, modeling and process monitoring are few of first choices one would seek. The complexity in the process makes it computationally expensive to estimate and visualize. Statistical analysis and development of a process map have been popular choices in estimating the workable domain for the process [1, 2].

Process monitoring being the other choice, various kinds of efforts have been made in attempt to visualize, track and adjust in real-time for various inconsistencies or deviations occurring during depositions. Song, Singh et al. [3] have incorporated a system of 3 CCD cameras and a pyrometer to track and in real time control the height and adjust the temperature of the meltpool.

Different from LMD, similar process monitoring strategies have been extensively studied for real time correction in welding and laser welding. The attributes such as weld pool diameter, surface of the weld pool etc. have been captured and in cases real time correction schema were established. Kovacevic et al. [4] incorporating a CCD and illuminating the weld pool with a laser were able to capture the surface detail and there by perform a real time correction during the process. Zhang et al. [5] while performing laser lap welding have used a spectrometer to analyze the plasma formed during welding to monitor the process and used a co-axially set up CCD camera to capture the weld pool. Incorporating image processing and edge detection techniques they have been able to identify defects happening during the process. Huang et al. [6] using an Infra-red camera have acquired temperature data and performed interference analysis on their

hybrid laser and TIG welding system. Similar attempts were performed using acoustic sensors, CCD cameras etc. in various unique methods to monitor the process and extract key attributes using image processing or calibrated setups[7-10].

In the current effort an infra-red camera was used to capture the deposition process and the gathered temperature data was processed using image processing techniques for edge detection thereby the liquidus region and solidus region were successfully identified.

Experimental Setup

A FLIR A615 camera has been used to perform the following studies. This was an industrial automation infrared camera with capabilities as listed in table 1. An IPG photonics YAG fiber laser and a Baystate technologies Model 1200 powder feeder were used to perform the deposition.

The camera was set at a 0.4 m distance from the deposit to visualize process from the front view. Thereby capturing the depth, front and tail ends of the meltpool.

Feature	**Specification**
Spatial resolution	0.69 mrad
Focal Length	25.4 mm
F-number	1
Imaging frequency	12.5 Hz to 200 Hz
Image resolution	640x480, windowing at high freq.
Temperature measured	3 ranges, -50 C to 2000 C (e=1)
Detector	Uncooled bolometer
Detector time constant	8 ms (typical)
Spectrum sensitive to	7.5 to 13 micron

Table 1. Specifications of the IR camera

Initial efforts were aimed at realizing the setup requirements and possible calibration steps to use the IR camera as a process monitoring tool. Later on the camera was used to see the trends in temperature during deposition, the size of the mushy zone while using LAMP lab's feedback system and acquired data was processed to identify the meltpool or the mushy zone and solidus regions in the deposit.

The IR camera measures the radiative power of a considered hot body which is later converted into temperature basing the Lookup tables, hence it is crucial that the right parameters be passed to acquire the accurate temperature readings. Laser metal deposition process is a very dynamic process and there are several aspects which result in significant and irregular changes in the input parameters required for the temperature conversion. The most pertinent of them being emissivity, for accurate measurement the spectral and thermal dependencies of the emissivity have to be identified and accounted for. For the initial set of experiments the thermal and spectral dependency was assumed to be negligent.

The camera performs only a gray body measurement, meaning the acquired data will be processed with a single emissivity (unless a pixel by pixel emissivity map is provided). Literature review states that the emissivity of metal oxide is higher than the respective metal and the emissive properties were favored by higher temperatures for solid phase. Therefore to rationalize the assumption of emissivity's temperature independence the acquisition has been performed in open atmosphere where the surface resulted in significant oxidation (considered oxide's emissivity at room temperature was around 0.9).

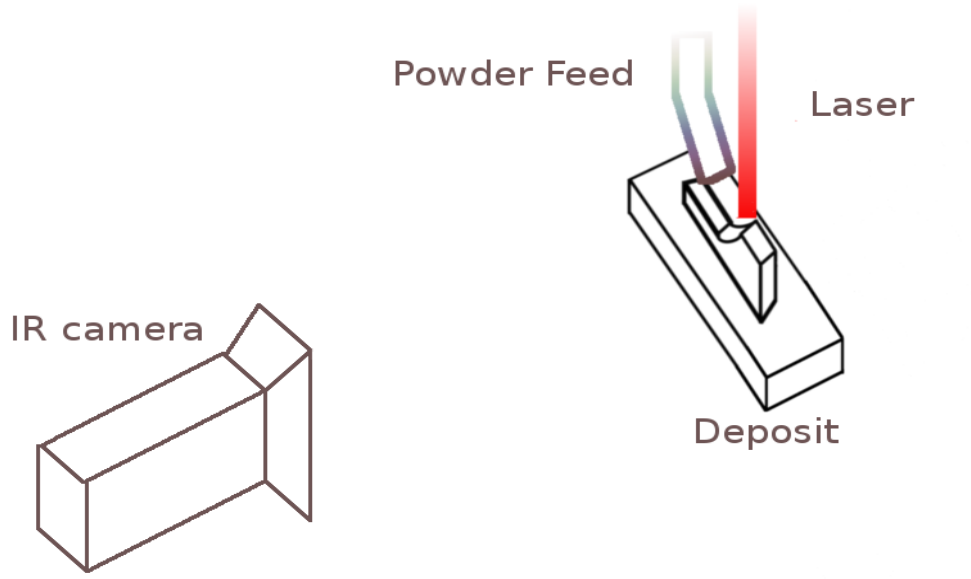

Figure 1. Schematic diagram showing the setup of the camera with respect to the deposit

Experimentation and Results

The deposition of stainless steel 316 was monitored using the IR camera. The emissivity was set to 0.95. The emissivity value was arrived at by averaging the emissivity values of the oxides of constituent elements.

A capture rate of 200 fps was set for thermal history acquisition, and other parameters, such as the atmospheric temperature, humidity, atmospheric reflective temperature and atmospheric transmission, were set as measured.

High-temperature region

The minimum cutoff temperature for this region was set as 100 degrees less than highest temperature occurring in every frame consecutively. The assumptions imposed while parameter selection create an unknown amount of error in the temperature readings acquired. Nonetheless, this experiment was instrumental in qualitatively identifying the size trends of this high-temperature region during deposition.

Deposition visualization

Using the iron color palette, a false color image was used to visualize the temperature data. The region above the minimum cutoff temperature also was visualized through the deposition. The green colored region in fig. 2 is the region containing temperatures in range of maximum in the frame and

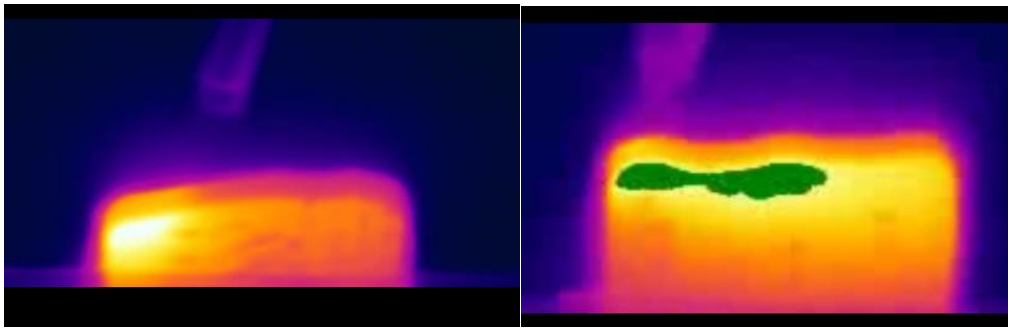

Figure 2. False color images used to visualize the deposition and highlight the high-temperature region at an instance during deposition

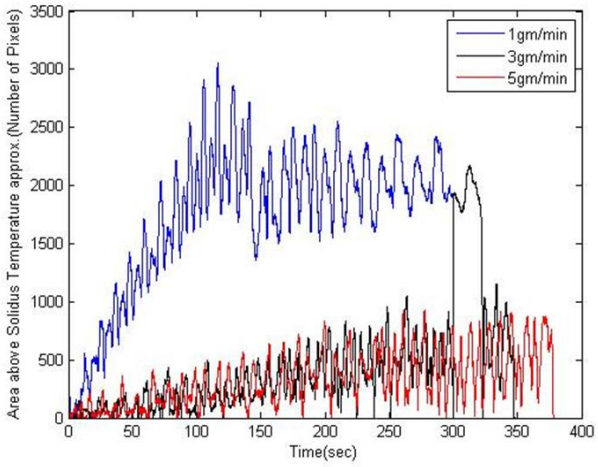

Figure 3. Size trends of the high-temperature region through deposition for variable powder feed rates and set points [11]

In order to ensure homogeneity throughout the deposition process, the optimum solution would be one that saturates the size of the high-temperature region. Though not a smooth saturation, the size of the high-temperature region stabilized around a certain range for a set of parameters. The

power was controlled by our in house power management system [11]. With varying powder feed rates the high temperature zone changed in area as shown in figure 3.

Image processing

There is a drop in emissivity when a metal undergoes phase transformation, i.e. when solid is melted into liquid there is a drop in the emissivity (meaning the reflectivity also goes up) [12]. As the ir camera reads the radiative power, it senses a decrease in temperature when such transformation occurs (as the temperature analyzed using a single emissivity value). The band radiance pertinent to the camera can be seen from the table 2.

SS 316		
Temperature	Emissivity [12]	Band radiance (7.5 to 13 micron)
Liquidus, 1400 C	0.3	4745 W/sq.m/sr
Solidus, 1377 C (oxidized)	0.95	1582 W/sq.m/sr

Table 2. Band radiance of Solid and Liquid phases of SS 316

This proves that the melt pool appears colder than it actually is, exploiting this phenomenon edge detection techniques have been chosen to identify the meltpool or the mushy zone in the thermographs. The change in emissivity can be seen from figure 5.

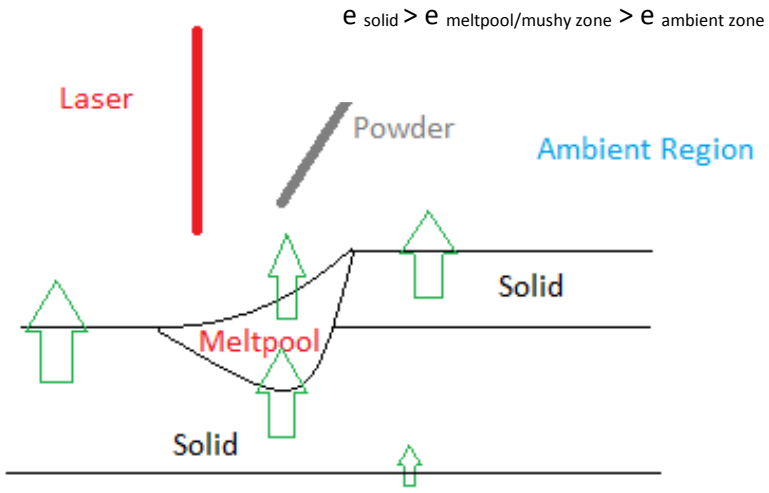

Figure 4. The boundaries and emissivity change trends in a thinwall during deposition

These transitions can be picked up by performing a gradient along the horizontal and vertical direction of the thermograph. Peaks (negative or positive depending on the direction) occurring when there is any of the depicted transition as shown in figure 4 can be seen in figure 5 and 6 as a height scale plot of gradients.

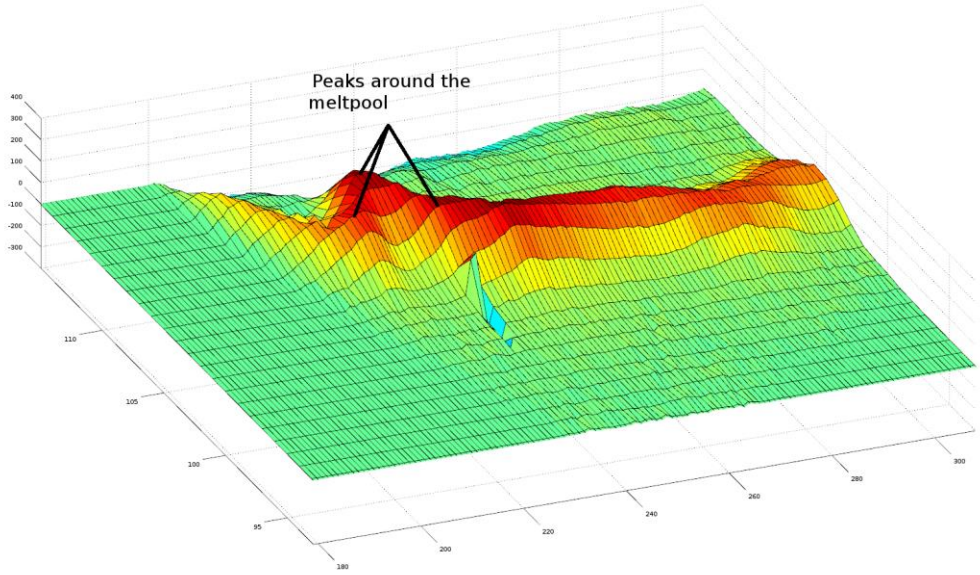

Figure 5. Peaks occurring around the melt pool and the top edge of the deposit when a gradient was performed along the vertical direction

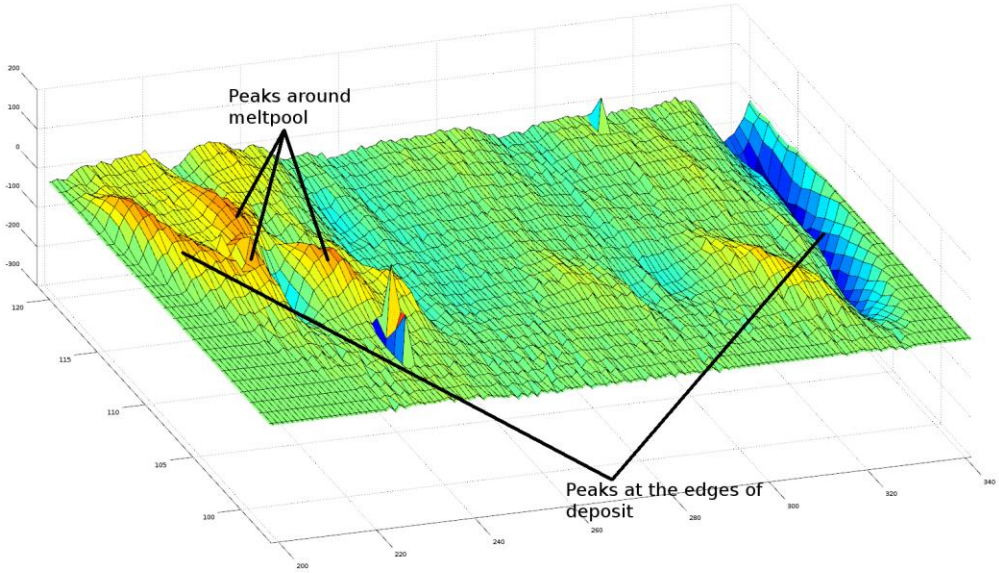

Figure 6. Peaks occurring at the vertical edges and around the meltpool region after a gradient was applied along horizontal direction

Edge detection

The sudden drop or rise in temperature while moving across these zones can be treated as an edge. Appropriately the Laplace edge detection technique has been chosen to identify the transitions in the deposit. The algorithm of this edge detection techniques is as shown in figure 7,

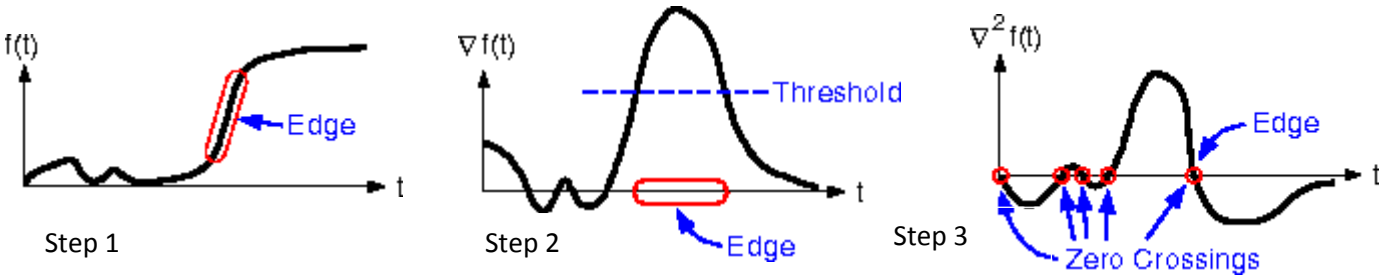

Figure 7. The steps in Laplace edge detection [13]

The Laplace edge detection technique targets the change in intensity of the signal and identifies the point of transition using the zero crossing points from the second degree derivative of the signal. The points of interest or the edges are identified using a threshold variance as the decision criteria in step 3 (from figure 7). This threshold value was chosen with the aim of detecting most significant changes [13].

Edge detection implementation

Steps involved during the image processing,

1. Moving Median

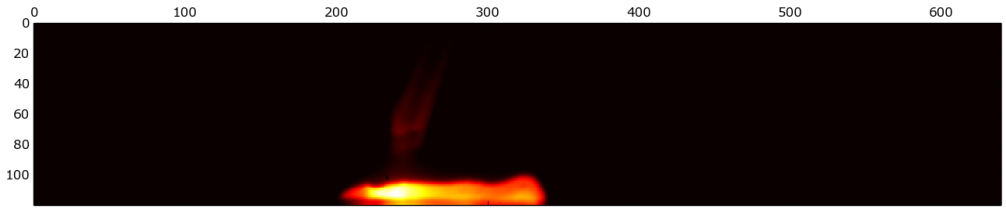

Figure 8. An instance during deposition after a moving median implementation

Moving median filters high difference variations in the frame by considering images in sets of 5. These would include the powder particle, which move rapidly in the frame and salt and pepper noise (figure 8).

2. Gaussian Blur and Laplacian Transform

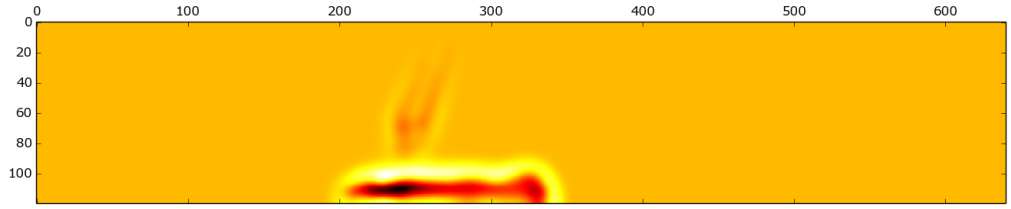

Figure 9. Gaussian and Laplacian transforms applied over the image (LoG).

A Gaussian blur would smooth the data within the image thereby ridding any minute variations from showing up while performing edge detection. The Laplacian transform performs an approximate second degree discrete differential over the image (figure 9).

3. Find zero crossings

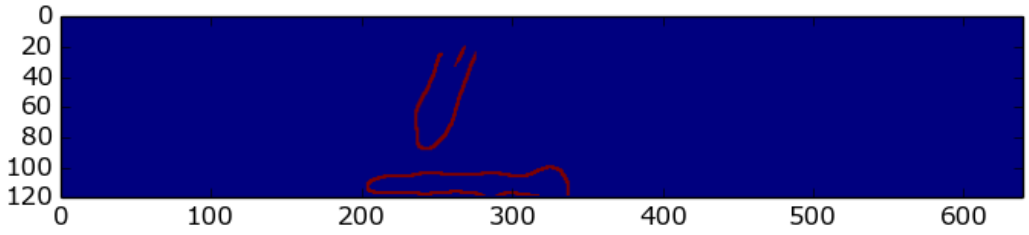

Figure 10. Sites of zero crossing in LoG with variance around the mean more than threshold value.

The LoG was then investigated for the zero crossings using a 3x3 kernel all over the image [13]. At sites where the variation around the zero crossing was more than the threshold value was designated as an edge. By doing so a binary image (as shown in figure 10) was made. The point to be noticed is that the melt pool boundary with in the deposit was not captured. The boundary or the edges of the deposit and the powder feed tube however were visualized.

The missing of boundaries within the deposit were attributed to the difference in temperature from liquid to solid to be less significant as compared to the difference in temperature from solid to air or liquid to air. Hence a localized search, limited to region within the deposit boundary was performed to identify the solid to liquid transitions.

4. Clarify image

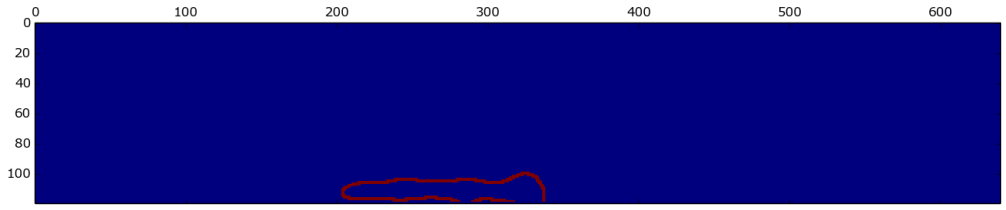

Figure 11. The image was clarified and only the deposit boundaries were retained

The powder feed tube was removed from the image and only the deposit boundaries were retained (as shown in figure 11). This image was later carried on for similar edge detection within the deposit to identify the meltpool boundaries.

5. Detect edges

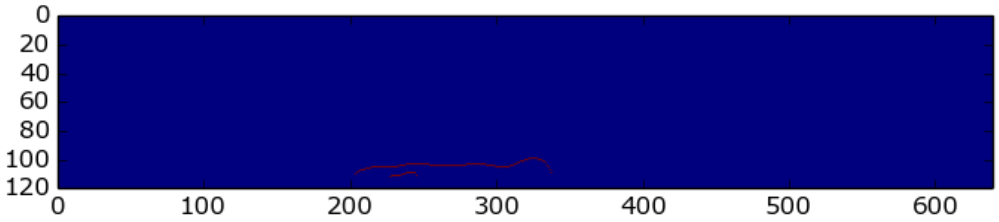

Figure 12. The top edge of the melt pool and the top edge of solidus region

The solidus region (previously called high temperature region) was marked in to the deposit. Fig. 12 shows a gap between the solidus region and the top edge of the deposit, affirming the claim that the meltpool/mushy zone is visible on the deposit in current setup of visualization.

6. Identify and process region around meltpool

A local edge detection was performed inside the deposit to identify the zero crossings and edges pertaining to the meltpool.

7. Mark meltpool and solidus region

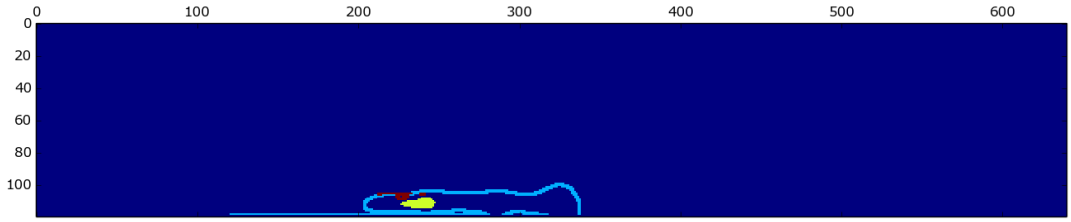

Figure 13. The meltpool/mushy zone (red) and solidus zone (yellow) boundary of the deposit (sky blue)

After completing edge detection and marking the solidus region, the corresponding areas were color coded and visualized in figure 13.

Instances during deposition

Following the above steps of processing various instances during the deposition were visualized for understanding.

Figure 14. Melt pool (white) solidus zone (yellow) and deposit boundary (red), left to right progression in deposition

Figure 14 shows instances where the first layer of deposit was being deposited. The effect of the mass as the material deposited increases the conduction increases and the region pertaining to solidus zone decreases in size.

(a)

(b)

Figure 15 (a) & (b). After steady state was achieved by the control system, left to right progression in deposition.

The above instance (figure 15 (a) & (b)) were instances the deposition process happened in a steady state and the size of the meltpool and the solidus region remained almost constant. The point to be noticed was that the size of meltpool region/ mushy zone increased with increasing deposited height, this can be explained by the increasing thermal resistance which is a consequence of the thin wall geometry.

Conclusions

An infrared camera was successfully been incorporated as a process monitoring tool to identify the solidus and mushy zone during deposition. The thermal history of a 316 SS deposition was acquired and processed. Keeping a gray body emissivity perspective the temperature data was filtered and processed using edge detection techniques. The deposit edges and the transitions between the liquid and solid phases were identified successfully. These regions were marked and the stabilization of the process was picked up.

Future work

Temperature co-relation between the regions of interest needs to be established and further emphasis needs to be imposed on decoding the constituents of the mushy zone. These explorative efforts need to be employed during deposition to identify various phenomenon while solidification.

Acknowledgements

This work was partially funded through NASA's Fundamental Aeronautics Program, Fixed Wing Project, under NRA NNX11AI73A. The authors would like to acknowledge William J. Seufzer and Karen Taminger of NASA Langley Research Center for their critical advice and mentorship. I would also like to thank the Department of Mech. Engg. at S&T and LAMP lab for their co-operation.

References

1. Liu JC, Li LJ Effects of process variables on laser direct formation of a thinwall. Opt Laser Technol 39(2):231-236. (2007)
2. Cao X, Xiao M, Jahazi M, Fournier J, Alain M, Optimization of processing parameters during laser cladding of ZE41A-T5 magnesium alloy castings using Taguchi method. Mater Manuf Processes. 23(3-4):413-418. (2008)
3. Song L, Bagavath-Singh V, Dutta B, Mazumder J Control of melt pool temperature and deposition height during direct metal deposition process Int J Manuf Technol 58:247-256(2012)
4. Kovacevic R. Zhang Y M, (1997) Real-time Image processing for monitoring of free weld pool surface, Jour of Manufac Scie and Engi 119:161-169 (2012)
5. Zhang Y, Zhang C, Tan L, Li S Co-axial monitoring of fibre laser lap welding of Zn-coated steel sheets using an auxiliary illuminant Optics, Optics & Laser Technology, 50:167-175 (2013)
6. Huang R S, Liu L M, Song G, Infrared temperature measurement and interference analysis of magnesium alloys in hybrid laser-TIG welding process, Materials Science and Engineering, A 447:239-243,(2007)
7. Lin L, A comparative study of ultrasound emission characteristics in laser processing, Applied Surface science, 186:604-610,(2002)
8. Gao J, Qin G, Yang J He J, Zhang T, Wu C, Image processing of weld pool and keyhole in Nd:YAG laser welding of stainless steel based on visual sensing, Trans. Nonferrous Met. Soc. China,21:423-428 (2011)
9. Saeed G, Zhang Y M, Weld pool surface depth measurement using a calibrated camera and structured light, Meas. Sci. Tech, 18:2570-2578,(2007)
10. Luo M, Shin Y C, Vision-based weld pool boundary extraction and width measurement during keyhole fiber laser welding, Optics and Lasers in Engineering,64:59-70, (2015)
11. Karnati S, Sparks T, Liou F,Vision-based process monitoring for laser metal deposition processes, Proceedings Solid Freeform Fabrication symposium 88-94 (2013)
12. Emissivity values as extracted on May 2014 from, http://www.raytek.com/Raytek/en-r0/IREducation/EmissivityTableMetals.htm, http://www-eng.lbl.gov/~dw/projects/DW4229_LHC_detector_analysis/calculations/emissivity2.pdf
13. Edge detection techniques as extracted on May 2014,http://www.owlnet.rice.edu/~elec539/Projects97/morphjrks/laplacian.html